FILAMENT CHANNEL STRUCTURES IN A Si IV LINE RELATED TO A 3D MAGNETIC MODEL

T. A. KUCERA[1,*], G. AULANIER[2], B. SCHMIEDER[2,**], N. MEIN[2] and J.-C. VIAL[3]
[1]*Code 682.3, NASA/Goddard Space Flight Center, Greenbelt, MD 20771, U.S.A.*
[2]*Observatoire de Paris, section Meudon, DASOP, URA 2080 (CNRS), F-92195 Meudon Principal Cedex, France*
[3]*Intstitut d'Astrophysique Spatiale, Unité mixte CNRS-Université Paris XI, Bâtiment 121, F-91405 Orsay Cedex, France*

(Received 30 October 1998; accepted 29 December 1998)

Abstract. A recent 3D magnetic model of filament support (Aulanier and Démoulin, 1998) has shown that specific morphologies derived from the model, based on SOHO/MDI magnetograms, match quite well with the observations of a filament observed in Hα and Ca II lines with the German telescope VTT in Tenerife on 25 September 1996 (Aulanier *et al.*, 1998, 1999a). Some predictions of this model concern the filament channel. To continue the comparison of model and data, we have investigated the same filament region observed in ultraviolet by the SOHO spectrometers SUMER and CDS. The elongated EUV fine structures in the filament channel observed in the Si IV 1393.76 Å line by SUMER have similar orientations and locations to features predicted by the model of Aulanier *et al.* (1999a). These regions are near the bases of field lines which tangentially join to the photosphere in so called 'bald patches' and are parts of large arcades above the filament channel. In addition, we consider the Si IV Doppler shifts in these structures and compare them to what might be expected from the model field structure. Our study also suggests that the filament has a very low opacity in Si IV, lower than that of the O V line observed by CDS.

1. Introduction

Démoulin and Priest (1989) and Démoulin, Priest, and Anzer (1989) proposed a theoretical model describing the magnetic field in filaments. The main hypotheses were that the dense plasma in filaments (which is observed in absorption in Hα) is supported against gravity in the magnetic dips of a twisted flux tube. Following this work, Aulanier and Démoulin (1998) constructed a 3D model of the magnetic field assuming a linear force free field in a theoretical highly sheared filament channel. The model describes a typical filament as well as its underlying lateral feet or 'barbs'. The results are in accordance with much observational evidence, such as the chirality rules found by Martin, Bilimoria, and Tracadas (1994) and the Hanle effect magnetic field measurements inside prominences by Bommier *et al.* (1994), summarized in the review of Démoulin (1998).

*SM&A Corp., Space Science and Engineering Division.
**Institute of Astrophysics, N-0315 Blindern, Oslo 3 Norway.

Solar Physics **186:** 259–280, 1999.

In Aulanier *et al.* (1998a) a magnetic field configuration, extrapolated with the assumptions of the model from a SOHO/MDI magnetogram, was compared to a filament channel observed in Hα. In the model the lateral feet are formed by a set of dipped field lines which connect down to the chromosphere/photosphere in small areas of parasitic polarity in the main bipolar background vertical field. The dips which connect to the photosphere are portions of larger field lines. The locations where such field lines are tangent to the photosphere (dip locations) are termed 'bald patches' (or BPs) in Titov, Priest, and Démoulin (1993). Their topological properties and their associated separatrices have been described in Bungey, Titov, and Priest (1996).

Further advances have been completed by Aulanier *et al.* (1999a). In that paper, the magnetic field is modeled in 3D under the 'magnetohydrostatic' assumption, using the basic equations derived by Low (1992). The field was extrapolated from an observed SOHO/MDI magnetogram. In this latter study, a detailed comparison of the model to Hα observations was performed, with an emphasis on the discussion of weak Hα blue shifts associated with computed magnetic dips above parasitic polarities. These dips were shown to correspond to Hα dark features, such as the filament itself and its feet, as well as some surrounding fibrils in the filament channel.

So far, the model of Aulanier and Démoulin has only been compared to MSDP observations in Hα and Ca II. In this paper we propose to compare the results of the model to EUV data. More precisely, we try to get some insight into the elongated fine structures, located in the filament channel beside the filament itself and observed in emission in Si IV. The question addressed in this paper is: are these features part of a classical chromosphere–corona transition region (CCTR) or not?

Moreover, the multi-wavelength observations in EUV of the filament itself lead us to consider the problem of the existence and nature of a prominence-coronal transition region (PCTR), which has been a matter of long debate (Engvold, 1989; Poland, 1990; Vial, 1990). Is there a PCTR 'sheath' surrounding the cool core or are filaments composed of isolated strands of different temperatures (Poland and Tandberg-Hanssen, 1983), What kind of flows exist in filament materials at transition region temperatures? These questions are important in understanding filament formation and support.

Previous to SOHO, most observations of filament flows in EUV have been done with the C IV 1548 Å line using the Ultraviolet Spectrograph and Polarimeter on the Solar Maximum Mission (SMM/UVSP) or the High-Resolution Telescope and Spectrograph. Blue shifts have been associated with filaments in both Hα and C IV (Schmieder, 1989 and references therein). Schmieder *et al.* (1984) report blue shifts in filaments, and Engvold, Tandberg-Hanssen, and Reichmann (1985) observed a transition between red and blue shifts on either side of the filament. Klimchuk (1987) claims that blue shifts relative to the average shift are a general characteristic of areas with low photospheric magnetic field, including filament channels.

In this paper we first describe the observations and initial data reduction. Section 3 describes the analysis of the filament and its surroundings. Section 4 presents the characteristics of the model, and Section 5 consists of a discussion of the findings, including a comparison of the EUV data with the model of Aulanier and Démoulin. In the final section we summarize our results and suggest improvements for future observations.

2. Observations and Initial Data Reduction

These observations were taken on 25 September 1996 as a part of SOHO Joint Observing Program (JOP) 17, 'The Dynamics of Solar Active Structures'. JOP 17 coordinated SOHO and ground-based instruments to study filaments. These included SUMER (Solar Ultraviolet Measurements of Emitted Radiation), CDS (Coronal Diagnostics Spectrometer), MDI (Michelson Doppler Imager), and EIT (the Extreme ultraviolet Imaging Telescope) aboard SOHO and ground-based instruments including the Vacuum Tower Telescope (VTT) in Tenerife and the Swedish Telescope at La Palma.

The filament observed was a long one, extending from S42 E32 to N8 W15. Preliminary results concerning this filament are presented in Mein *et al.* (1998) and Aulanier *et al.* (1998b). Later in the day its southern portion erupted, but the northern section studied here remained (Schmieder *et al.*, 1997b; van Driel Gesztelyi *et al.*, 1997, 1998).

2.1. SUMER

The capabilities and in-flight performance of the SUMER spectrometer are described in detail by Wilhelm *et al.* (1995, 1997) and Lemaire *et al.* (1997).

The SUMER observations consisted of a series of half-hour rasters taken from 7:22–12:00 UT, initially centered at $28''$, $-140''$ with adjustments for solar rotation. The observations were taken with the $1 \times 120''$ slit across the top (south) band of detector B. As usual, the slit was oriented north-south and rasters were taken by shifting the pointing eastwards. The first raster covered a $150''$ field of view east-west with $3''$ raster steps. Eight subsequent rasters were taken over a $75''$ field of view with smaller $1.5''$ raster steps.

The exposure time for all SUMER observations was 35 s. The resolution in the north-south direction was $1''$ pixel^{-1}. Because of the position of the telescope aperture there is no data in the top 30 pixels of the detector at the wavelengths we observed (see below), so we have only 90 pixels ($90''$) of data in the north-south direction.

Spectral resolution of SUMER is about 0.052 Å with 0.043 Å pixel^{-1}. Data were returned from two 50 pixel spectral bands centered on the Si IV line at 1393.76 Å and the O V line at 1371.29 Å. In this study we use only the Si IV line because of the low signal-to-noise ratio in the O V data.

The flat-field correction was done in flight using the flat field obtained on 24 September, the day before the observations. Geometrical distortions of the detector were removed using the destretching procedure of Moran (1999).

To produce full Doppler maps the SUMER Si IV spectra were fit by a Gaussian at each point. The count rate in individual pixels was often quite low (< 10 counts pixel^{-1}), so there was not enough signal to fit the small line immediately redward of the much brighter Si IV line. It was not possible to produce an absolute wavelength calibration, so the mean over the entire Si IV map was set to -7.8 km s^{-1}, a typical average red shift in Si IV. All Doppler values from the SUMER data set cited in this paper have been normalized in this way. The -7.8 km s^{-1} value is based on work by Chae, Yun, and Poland (1998) who give an average value of -7.8 ± 1.5 km s^{-1} for the quiet-Sun Si IV Doppler shift. Brekke, Hassler, and Wilhelm (1998) give -7 ± 2 km s^{-1} for the Si IV velocity. To be conservative we can include both these values by assuming the uncertainty is about 3 km s^{-1}. We emphasize that this does not affect the relative uncertainties of the values at different locations.

2.2. CDS

The CDS instrument and initial results are described by Harrison *et al.* (1995, 1997). As with the SUMER observations, the CDS observations consisted of an initial large field raster ($121 \times 240''$) followed by a series of smaller field rasters. The observations were taken from 07:41–12:00 UT. They were initially centered at $53''$, $-120''$ with later adjustments for solar rotation. The first raster covered a $244'' \times 240''$ field of view with $2''$ raster steps east-west. This was followed by ten $121'' \times 240''$ rasters taking 23 min each with 59 raster steps. Exposure time was 10 s. We used the $2'' \times 240''$ slit oriented, as usual, north-south. Spatial resolution along the slit was $1.68''$ pixel^{-1}. Lines observed included He I at 584.33 Å, and O V at 629.73 Å as well as a number of coronal lines (in Si IX, Mg IX, and Mg X). CDS He I and O V images are presented in Figure 1.

2.3. MDI

Near the time of our observations on 25 September 1996 MDI took two magnetograms, on at 07:40 UT and the other one, a five minute average map, at 12:53 UT (see Figure 2); both have a pixel size of $2''$. The first corresponds to the start of our program with the large, raster, the last is done nearly one hour after the end of our observations. Single magnetograms are limited by the shot noise to about ± 20 G and 5 min average maps to about ± 12 G (Hoeksema, 1998, private communication). The evolution of the small polarities is quite significant between these two times in our field of view principally near the feet of the filament (Aulanier *et al.*, 1999a).

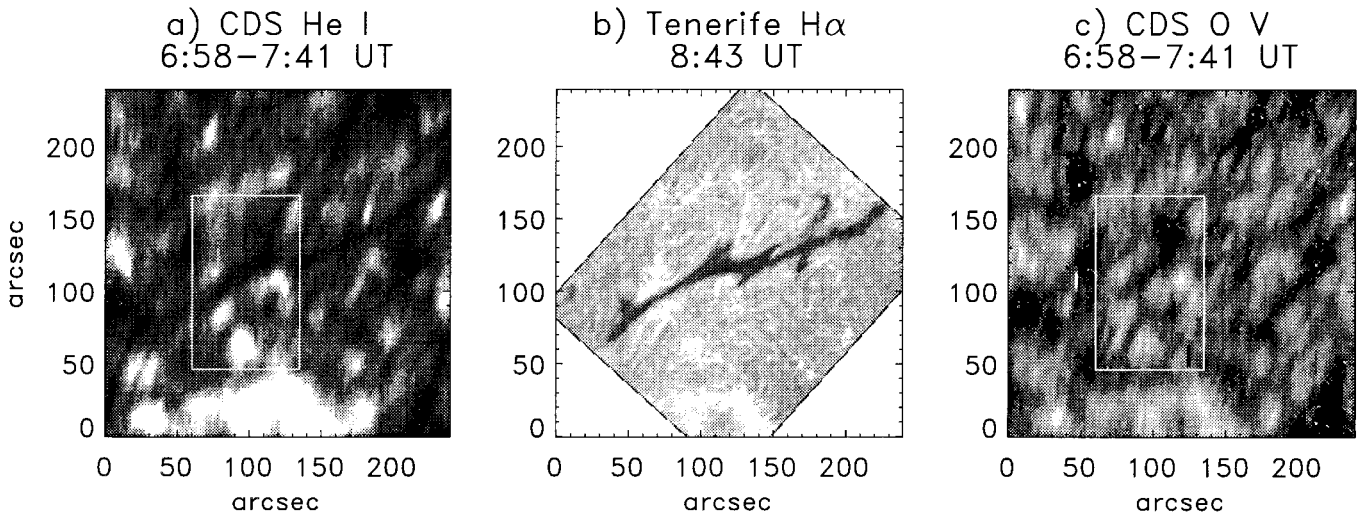

Figure 1. Filament observed on 25 September 1996 in (a) He I (CDS) at 06:58–07:41 UT, (b) Hα (Tenerife VTT/MSDP) at 08:34 UT, and (c) O V (CDS) at 06:58–07:41 UT.

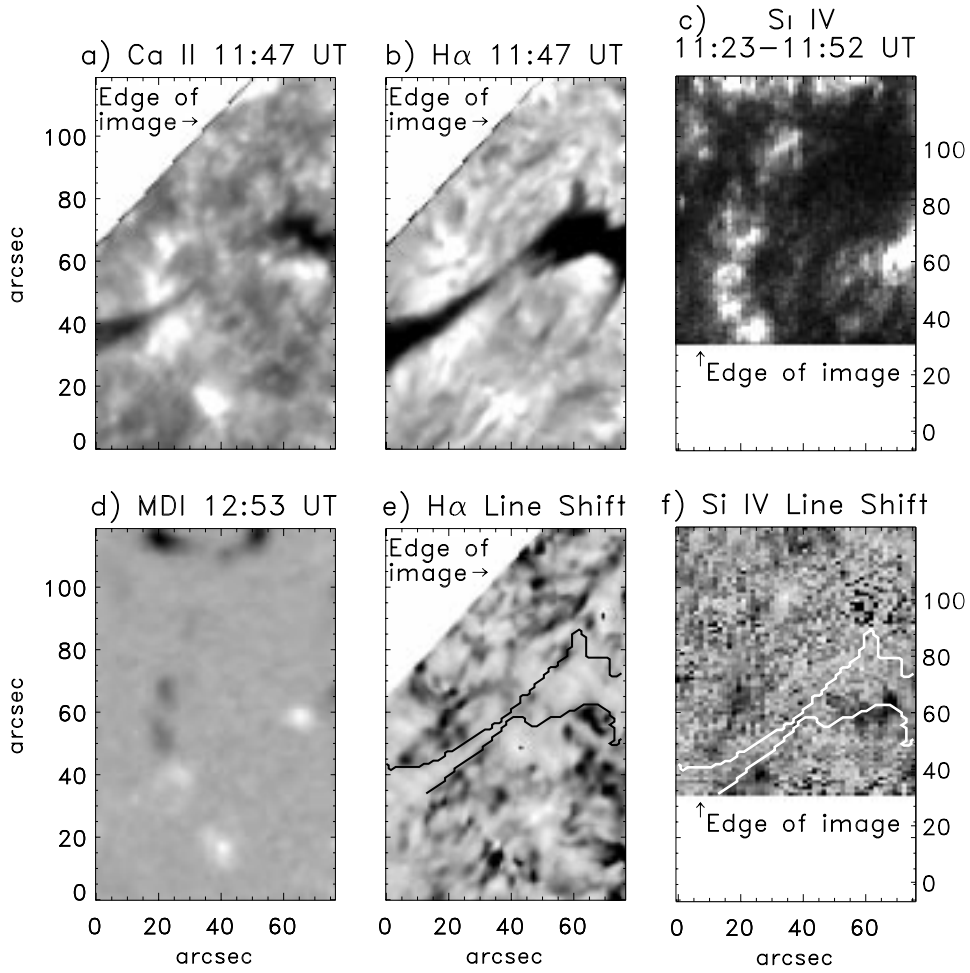

Figure 2. Portion of the filament of 25 September 1996 in: (a) Ca II line at 12:14 UT observed with the MSDP, (b) Hα at 12:14 UT with the MSDP, (c) Si IV line at 11:23–11:52 UT by SOHO/SUMER,(d) MDI longitudinal magnetic field at 12:53 UT, (e) Hα velocity at 12:14 UT with the MSDP, (f) Si IV velocity 11:23–11:52 UT by SOHO/SUMER (average velocity set to -7.8 km s^{-1}). The velocity maps are overlaid by the contour of the filament in Hα. Blue shifts are light, red shifts dark. The fields of view of the SUMER and VTT images do not cover the entire areas shown.

2.4. MSDP

The main ground-based observations used in this investigation were obtained with the Multi-channel Subtractive Double Pass (MSDP) spectrograph mounted on the German telescope (VTT) at the Teide Observatory in Tenerife. The details of MSDP data reduction are described by Mein (1991). Nine images of the same solar area were recorded simultaneously in nine wavelengths of the Hα profile on a 1024 $\times$ 1024 pixel CCD camera. By using 200 successive steps across the disk we scanned

two strips of 170″ × 600″ every 34 min. The pixel size is 0.43″ for the recording and 0.25″ for the output maps. The MSDP simultaneously observed the selected strips in Hα and in the *y* line of Ca II. The Hα profile is determined at each pixel of the field. Doppler shifts and intensity fluctuations are derived at different distances from line center. The Hα images of the filament presented here are computed at ±0.5 Å, the Ca II at the line center. The filament was tracked all day from 08:43 UT to 17:04 UT (Mein *et al.*, 1998).

2.5. CO-ALIGNMENT

Co-aligned maps from CDS and the VTT on Tenerife are shown in Figure 1. The large plage at the bottom of the CDS field-of-view is well co-aligned with the facula in Hα. The SUMER (box in Figure 1) and CDS maps were aligned using the network and the small plage regions visible in the large SUMER raster and the CDS data. These observations were obtained during the last week before the SUMER pointing mechanism started to have problems, and a large correction has to be applied to the SUMER field of view, a shift by almost 33″ eastward, to align the two data sets.

The EUV data have been coaligned on a finer scale with ground-based images, the Hα and Ca II data from the VTT in Tenerife, by feature-tracking techniques using data from the Ca II line center which are taken coincidentally and co-spatially with Hα data (Figure 2).

Commonly the network structures correspond to magnetic concentrations and appear bright in photospheric lines, in Hα and even more in Ca II lines (Malherbe *et al.*, 1987). The network also appears in transition region lines such as Si IV and C IV. The correlation between faculae observed in Hα and bright regions in C IV could reach 0.6 and the correlation over the whole field of view (4′ by 4′) was found to be around 0.350 by using SMM data (Malherbe *et al.*, 1987).

Therefore, the alignment was performed using bright network structures in both Ca II and in transition region EUV lines from Si IV and O V. MDI data and Ca II were then coaligned easily because of the good correspondence between Ca II intensity and magnetic field strength. The coalignements were performed on two data sets, the ones closest in time to the MDI observations (nearly one hour after the first magnetogram and one hour before the second magnetogram). We mainly show the second set of data, obtained between 11:42 UT and 12:51 UT (Figure 2).

3. Analysis

3.1. Intensity structures

In Figure 1 we can distinguish in the CDS images the different features visible in Hα. The filament appears as a long, thin, dark region in He I, comparable to the Hα. This is quite normal because of the similarity of the temperature formation of these two lines (10^4 K). In O V the filament is still visible but the contrast is less. Three feet are clearly visible in this field of view.

In the SUMER field of view, limited to the box in Figure 1, only one of the feet is visible: the central one, which is at the west edge of the box. As was mentioned in Section 2, only 90″ of the SUMER slit is available, reducing the field of view of SUMER further. The filament in Si IV is not detectable and has the same contrast as internetwork structures (Figure 2). The filament lies between negative (north) and positive polarities (south) as usual along the magnetic inversion line (see Figure 2(b)). Close to the foot of the filament (western side of the images) a very bright feature in Si IV is visible. It corresponds to a positive polarity in the MDI image. Close to the western edge of the field of view there is a suggestion of some negative polarity. In fact, the negative polarity does exist in a larger field of view and evolves during the day. This parasitic polarity was referred to as 'N1' in Aulanier *et al.* (1999a) where it was related to the presence of the lateral foot seen in Figure 2(c). However, we have no magnetograms to confirm the motion of these polarities during our observations or to compare with the changes of the Si IV bright regions.

In the He I box (Figure 1(a)) we see a series of small brightenings on the eastern side of the filament oriented north-south in a C-shape. These correspond to the network and are apparent in SUMER and MDI observations as well (Figure 2). The 'C' shape is outlined in Figure 3, described in Section 3.2.

One noticeable feature of these data is that the filament is more easily seen in the O V data than in the Si IV data. This is in part because there is less background emission to be absorbed in many parts of the Si IV image. However, there is also a difference in the amount of absorption in the area where the filament crosses the 'C'. This indicates that the Si IV line at 1393.73 Å is more optically thin than the O V line at 629.73 Å. The explanation for this very likely lies in the relative abundances of the two species. The strength of a resonance line depends on the oscillator strength, the inverse of the Doppler width, and the ground populations. If we assume that the lines are being formed at the peak of the contribution temperature, the ground populations then depend on the local electron densities, which are expected to be slightly higher in cooler regions in which Si IV is formed. In the case of the Si IV and O V lines, the oscillator strengths are comparable and the Doppler widths are inversely proportional to the wavelengths so that the optical depth of Si IV would actually be expected to be higher than that of O V. Thus the different behaviors of these lines are best explained by the respective abundances of O and

Si, which are in a ratio of 24 in the photosphere and 6 in the corona (Feldman, 1992; Meyer, 1985). (Note that we do not consider the possibility that the O V line has strong absorption by the Lyman continuum in the filament.)

This observation is consistent with the model of Chiuderi-Drago, Engvold, and Jensen (1992), who determined that filaments seen on the disk in C IV are likely to be transparent, although prominences seen off the limb may not be.

3.2. FINE STRUCTURES IN Si IV

The model of Aulanier and Démoulin, discussed in Section 4, makes predictions concerning the fine structures near the filament. Thus we consider the fine structures observed in the Si IV images.

In order to sharpen the image, we used the 'madmax' procedure (courtesy of O. Koutchmy and S. Patsourakos). This function looks for octodirectional maxima of convexities: it determines a multi-directional maximum of minus the second derivative, using 8 directions and a double step (Koutchmy and Koutchmy, 1989). As it amplifies convex points, this method has the effect of detecting discontinuities. The result is shown in Figure 3.

In the 8 small SUMER rasters the evolution of the bright regions could be followed. The C-shape brightening (on the left in Figure 3) is always visible with small variations in brightness. There is also a western bright feature near the foot where the filament material is connected with the chromosphere. This structure changes shape and location as the filament foot in Hα changes. To its south-east are elongated, diagonally-oriented bright structures.

These bright threads evolve during the day of 25 September, but their lengths and orientations are not much affected by the variations of intensity in the Si IV line. Time sequences of SUMER images show that the typical time scale for the brightening/dimming of these features is on the order of an hour.

Some of these threads overlay the filament region, and some are located in the filament corridor, e.g., in the southern part of the foot. These latter form a shape like crab pincers, also shown in Figure 3.

The temperature of formation of Si IV is about 100 000 K. In general, the fine structures could be structures of the transition region or threads belonging to the filament. In Section 4 we consider the possibility that some of these structures are material heated along the field lines in the filament corridor.

3.3. VELOCITY FIELDS

Doppler maps of Si IV and Hα are shown in Figure 2. Because we could not do an absolute wavelength calibration for these data, the average Doppler shift over the whole map has been set to a typical value for Si IV in the quiet Sun, -7.8 km s^{-1} (see Section 2.1).

Although, as is generally the case, the blue-shifted filament can be clearly seen in the Hα Doppler image, the filament does not show a clear signature in the

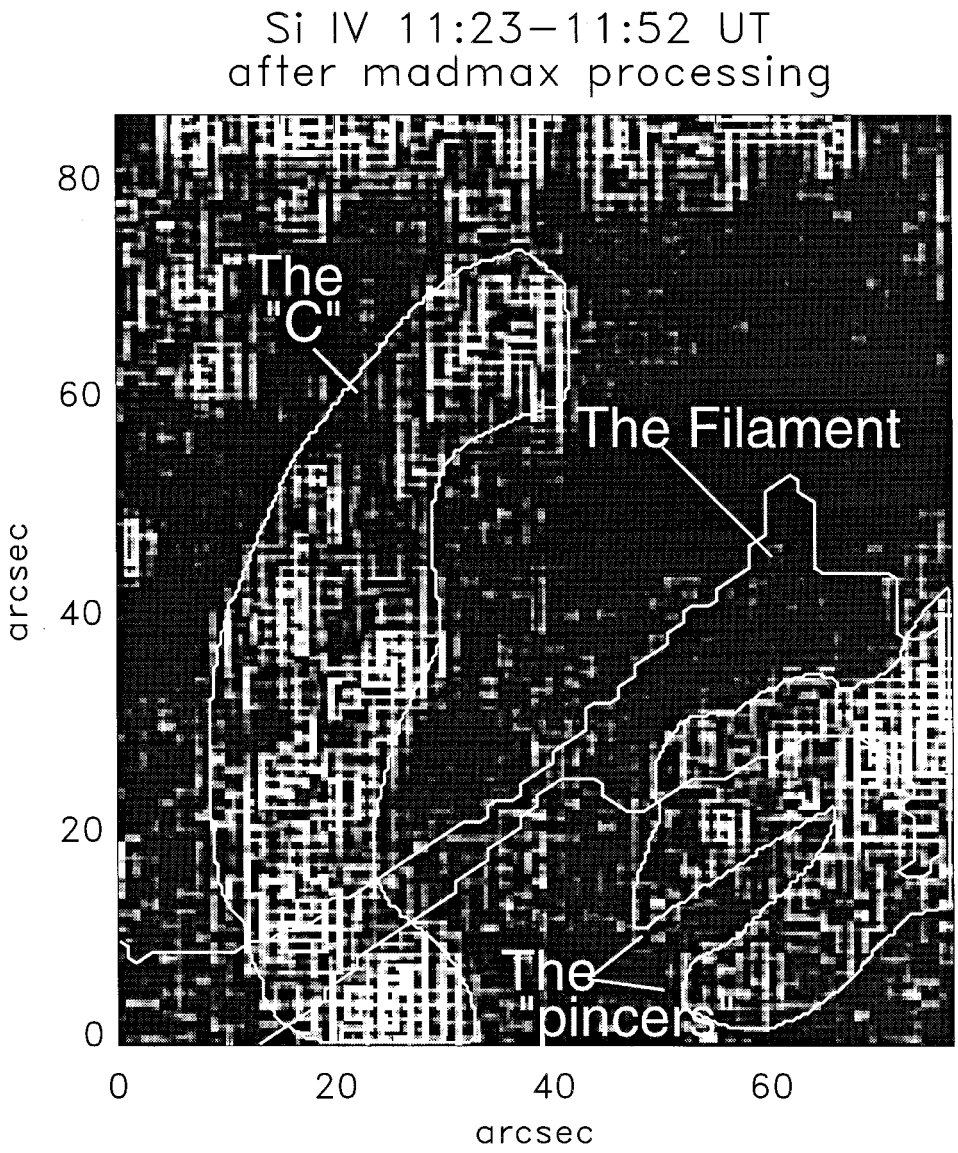

Figure 3. Si IV map at 11:23–11:52 UT image with special data processing. The contours of the filament, the 'C', and the bright region to the west (the 'pincer') are labeled.

Doppler shifts of the Si IV data. The obvious velocity features in the SUMER data consist of the bright network, which is clearly red-shifted, as has been observed before (e.g., Klimchuk, 1987). The flux from the filament area is not significantly different from that of other areas near by without filament or network, as is shown in Figure 4. This figure shows line profiles of combined data from (1) filament areas without network, (2) an area north of the filament without network, and

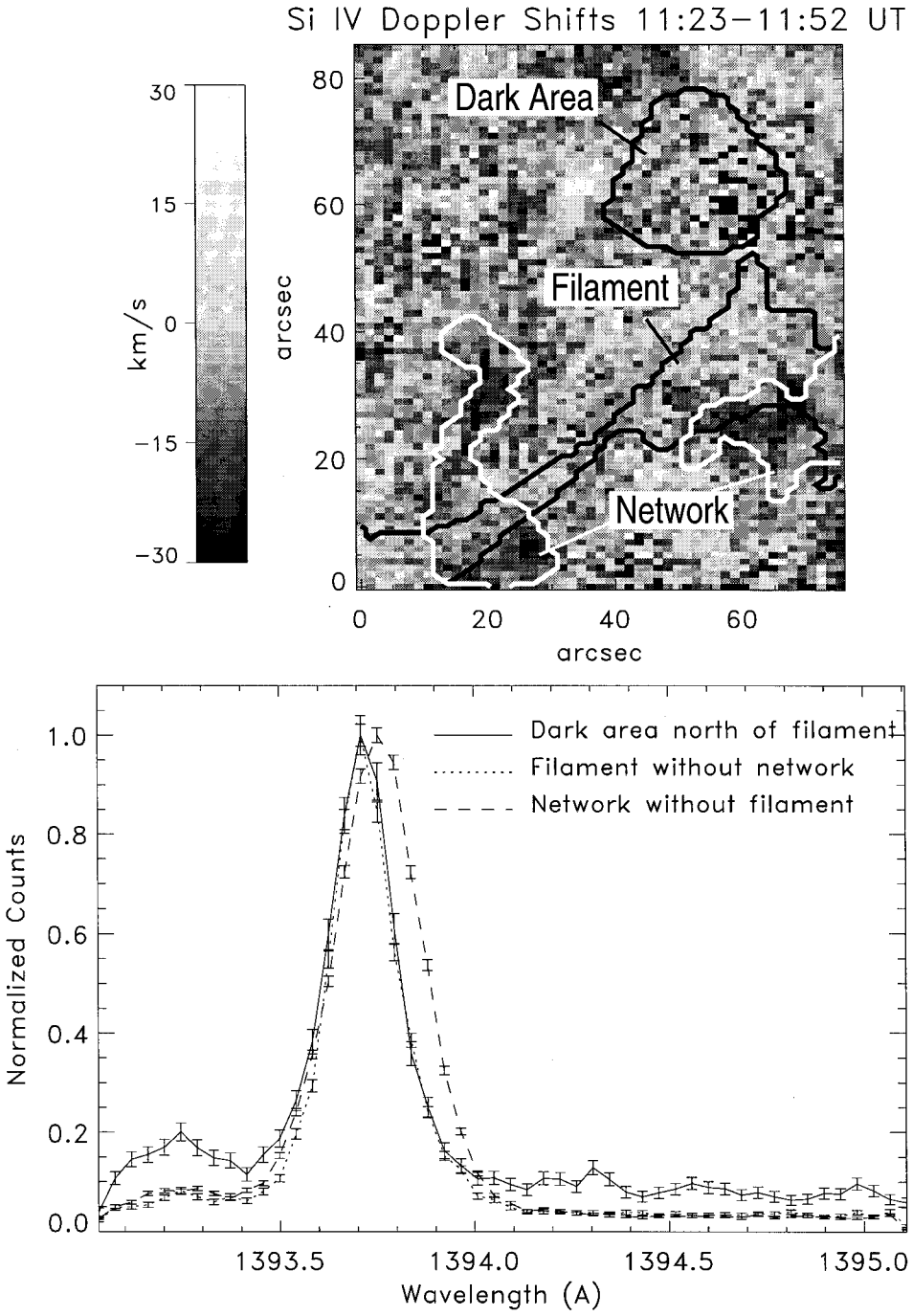

Figure 4. Line profiles of filament, bright network, and an area that is not filament or network. The amplitudes of the lines have been normalized to one to make them easier to compare.

(3) the network without filament. The line profiles were constructed by summing the fluxes over the areas shown in Figure 1. We also tried normalizing the points before summing to prevent overweighting brighter points but got essentially the same results. Areas where the filament and network overlap have velocities in between the averages for the network and filament. It is difficult to tell if we are seeing a combination of the signals from the filament and the network or only the filament channel.

We also considered the velocity properties along the fine structures (the 'pincer' visible to the south-east of the southern foot observable in the SUMER data. Spectral profiles were calculated along the features by rotating the image so that the features were vertical and summing in the vertical direction over 15 pixels to reduce the noise. Figure 5 shows the profiles summed parallel to these features in the two selected boxes. The error bars shown in the plots are relative errors. As mentioned in Section 2.1, there is an uncertainty in the overall offset of the velocities of ± 3 km s^{-1}.

In general, the data are rather noisy, and it is hard to establish a pattern for the small structures. If anything, there does seem to be a general trend towards brighter areas being more red-shifted. However, there are exceptions, including the southern part of the 'pincer' feature at the south of the filament, which is blue-shifted relative to its surroundings. A bright, blue-shifted feature is contrary to the general pattern of bright features being more red-shifted. We will relate this observation to possible evaporation of the plasma in the next sections.

4. Model of the Filament Channel and Sites of Energy Release

In this Section we compare UV observations of the filament channel with computed field lines in the vicinity of the filament, using the 3D model of Aulanier *et al.* (1999a). Figure 6 shows the basic components of the model near the filament feet. The magnetic field lines forming the feet are extensions of lines which arch over the lines containing the main filament material. The field lines of the feet come down to the surface near small areas where the magnetic polarity is opposite the main field on that side of the filament neutral line. The field lines which are actually tangent to the photosphere form the separatrix where the magnetic field reverses direction. The curve along which the separatrix intersects with the local neutral line in the photospheric plane is the 'bald patch' (or BP). Over the BP the fields form dips in which material is expected to collect, just as in the main part of the filament. Below we discuss the physical basis for the predictions relating to Si IV emission and compare the predictions with our observations.

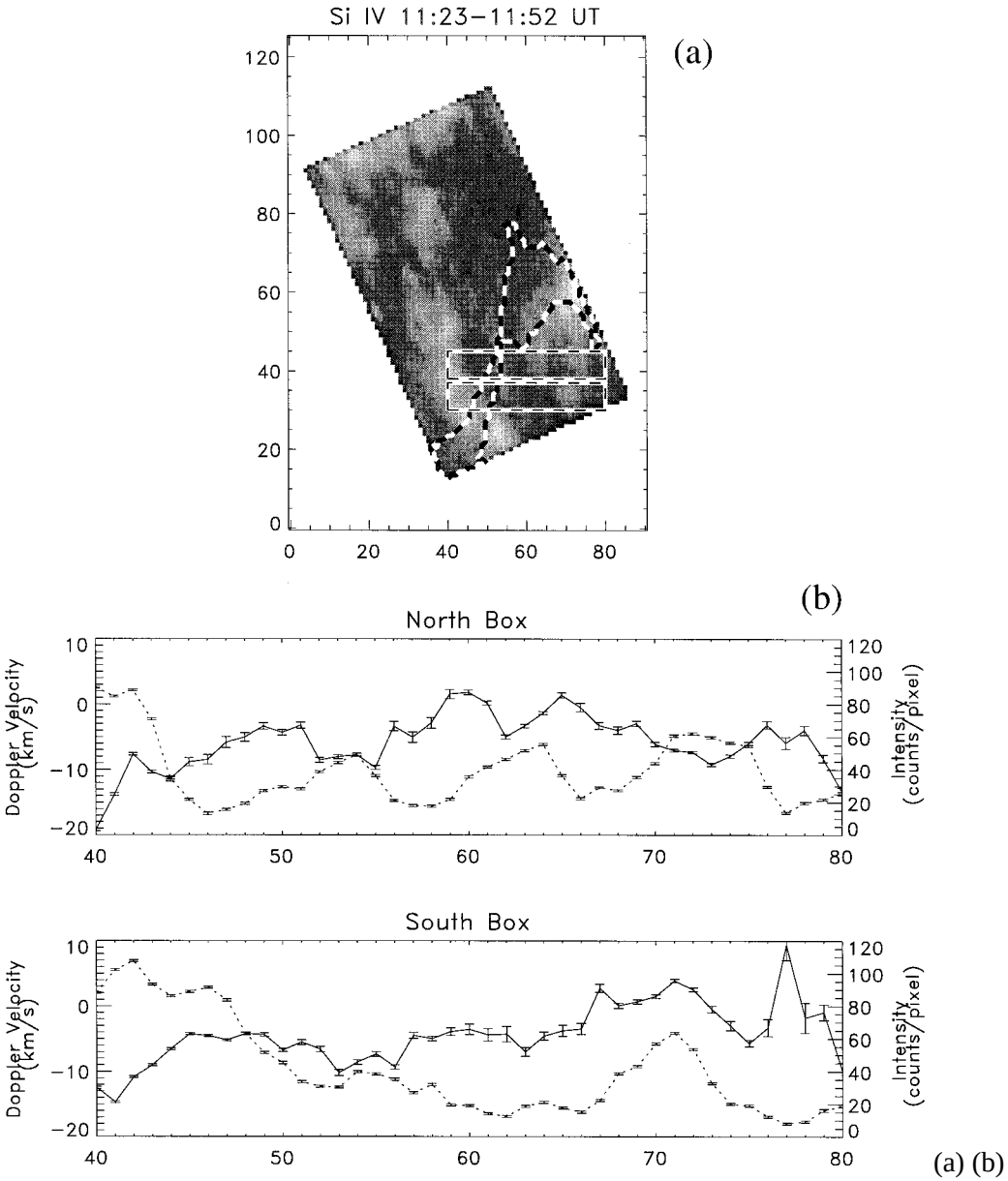

Figure 5. (a) Si IV map showing the two boxes where the fine structure analysis is done. (b) Curves showing the intensity and Doppler shift with location. The solid line is velocity, the dashed line is intensity.

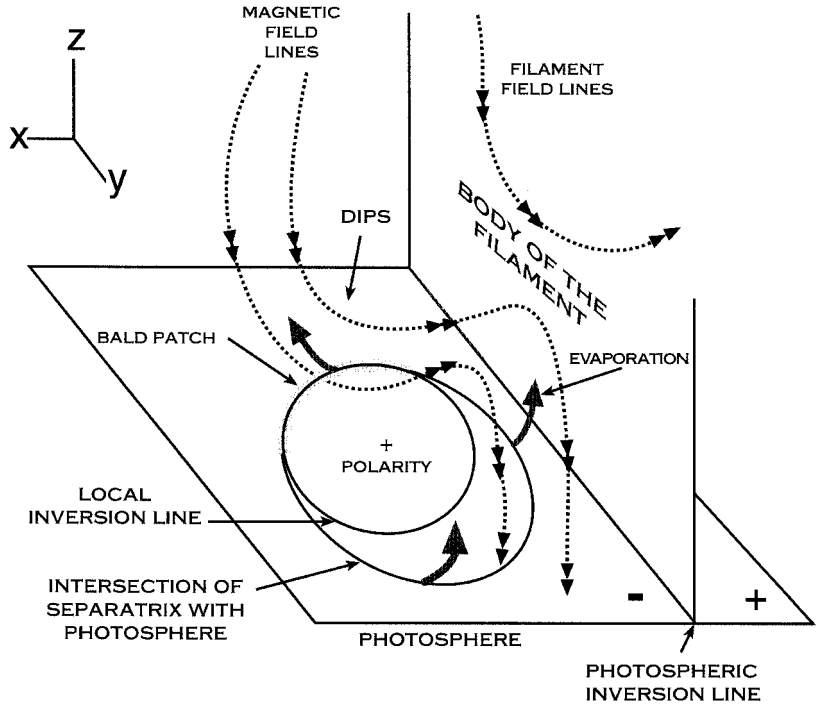

Figure 6. Sketch in 3D of the model of the filament feet discussed in Section 4. The dotted lines are the magnetic field lines. Those associated with the parasitic polarity form the filament feet. The field lines tangent to the photosphere form the separatrix. The figure shows the intersection of the separatrix and the photosphere. The intersection of the separatrix and the local magnetic neutral line is the bald patch ('BP', shown by the thick, grey curve). The magnetic field forms dips above the BP, in which Hα absorbing material collects. The whole curve formed by the intersection of the separatrix with the photosphere may be heated resulting in emission on Ca II while the plasma along the whole separatrix surface may be also heated, and thus emit in Si IV. Gentle evaporation may occur in the field lines anchored in the BPs, so that upwards plasma flows along these field lines can be observed. This evaporation is shown by the grey arrows.

4.1. LARGE FIELD LINES ROOTED IN 'BALD PATCHES'

In this paper, the magnetic field is computed with the same method used in Aulanier *et al.* (1999a), from the SOHO/MDI magnetogram observed at 12:53 UT. Figure 7 shows some of the modeled field lines in 3D. Apart from the dipped portions some field lines (which can be correlated to the filament, its feet, and some dark Hα fibrils), a sample of long field lines anchored in the photosphere onto some BPs are present in the filament channel. Because such a field line is exactly rooted in a BP, it is in fact part of the separatrix surface associated with this BP (Bungey, Titov, and Priest, 1996). The portion of these field lines lying below 15 Mm is drawn darker in Figure 7 than their remaining part at high altitudes. Our model shows that these field lines form sheared arcades overlaying the twisted flux tube (where the filament material is in equilibrium in magnetic dips). Such arcades are

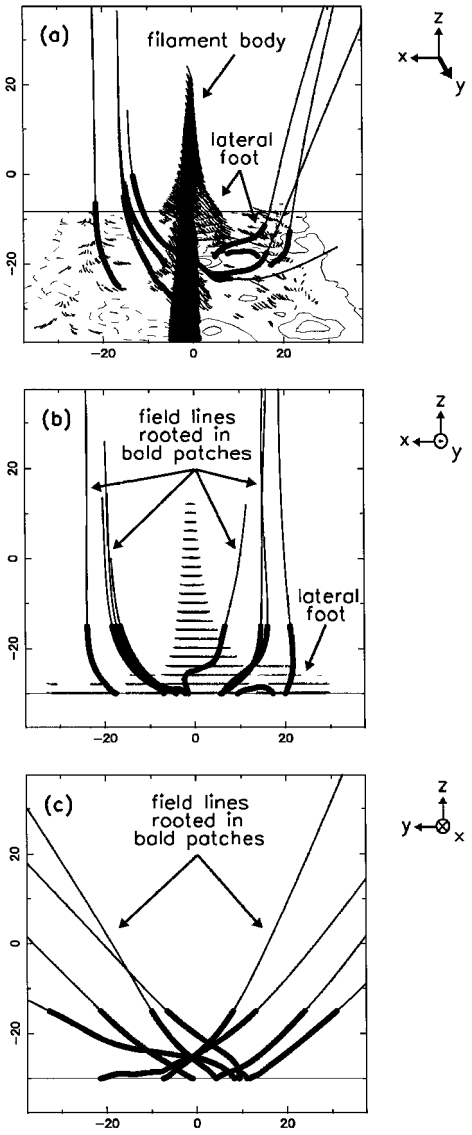

Figure 7. Side views of the 3D magnetohydrostatic prominence model (which is viewed from the top in Figure 8(c)). In these plots z is upwards, y is along the filament, and x is in the remaining direction, parallel to the photosphere and perpendicular to the filament axis. The plots depict areas 75 Mm $\times$ 75 Mm. (a) A view along the filament from above the photosphere. The thin solid lines on the photospheric plane correspond to isocontours of the vertical magnetic field from SOHO/MDI of 8 and 24 G, and the dashed lines to -8 and -24 G. Plot (b) shows the same view as (a) but looking more parallel to the photosphere (along the y axis). Plot (c) is a view in the x direction, perpendicular to the filament axis. In both (a) and (b) the small thin lines correspond to the dipped portion of the field lines forming the filament, which are drawn up to a depth of 300 km (equal to the typical pressure scale height in filaments). The dips are computed at regular intervals: $\Delta x = 0.75$ Mm, $\Delta y = 1.5$ Mm and $\Delta z = 2$ Mm. Plot (c) does not include the filament for reasons of clarity. In (a), (b), and (c) the long lines correspond to the bottom of large sheared field lines forming the arcades over the filament body, and anchored at bald patches (BPs). The portion of these lines lying between the photosphere and the altitude of 15 Mm are drawn darker that their remaining part above 15 Mm. Notice on (c) that the bottoms of some of these field lines are very flat on a horizontal extent of typically 10 Mm, departing from the BP from which they originate.

usually observed at high altitudes in soft X-rays (e.g., by *Yohkoh*, see Martin and McAllister, 1996).

Figure 7(c) shows that such close-to-the-filament field lines are very sheared; more precisely, they are nearly parallel to the filament axis. Moreover, the portions show the thickest lines (below 15 Mm), which are close to the BPs, are bent strongly parallel to the photosphere, so that these parts of the field lines are nearly flat, at least close to the BP. The angle θ of the field lines below 15 Mm with the photosphere is typically $0 \leq \theta \leq \pi/6$.

4.2. HEATING IN BP SEPARATRICES?

Low and Wolfson (1988), Vekstein, Priest, and Amari (1991), and Aly and Amari (1997) have shown that strong currents can be generated at BP separatrices. Billinghurst, Craig, and Sneyd (1993) have studied the conditions of current sheet formation at BP separatrices in the case of asymmetric 2.5D configurations. However, contrary to Low and Wolfson (1988), they have shown little evidence of vertical current sheet formation at the BP when photospheric shearing motions are present. However, Aly and Amari (1997) have shown that a vertical current sheet can still be present above the BP if there exists a neutral X-point resulting from photospheric converging (or diverging) motions.

The physics of current accumulation and dissipation is expected to be significantly different between BP locations and the corona, mainly due to the high density of the plasma at the photospheric/chromospheric level. One of these effects is to reduce the validity of line-tying at the BP. This point has been numerically studied by Karpen, Antiochos, and DeVore (1991) and further discussed by Billinghurst, Craig, and Sneyd (1993). In a topological context, this effect broadens the BP separatrix, forming a quasi-separatrix layer (QSL). The possible formation of a current layer in QSLs is still under debate, though Démoulin *et al.* (1996) have given some positive arguments for it.

The model of Aulanier *et al.* (1999a) does not directly address these issues. However, from the studies discussed above we expect that strong currents should be present in the computed BP separatrices. These currents probably lead to ohmic dissipation or magnetic reconnection. Whichever of these processes of energy release are at work, the plasma will be strongly heated. Then the field lines lying in the separatrix surface of the BPs can be observed as UV or X-rays loops. We expect these assumptions to be valid, as such a correlation between computed field lines rooted in BPs and elongated soft X-rays brightenings has already been achieved by Aulanier *et al.* (1999b) in the context of an observed subflare.

4.3. PLASMA EVAPORATION IN THE CONTEXT OF ENERGY RELEASE

As energy is released along the BP separatrix, accelerated particles are expected to hit the chromospheric layer, forming bright regions such as flare kernels. Their locations have been correlated to the intersection of (quasi-)separatrices with the

chromosphere by many authors, such as Démoulin, Hénoux, and Mandrini (1992), Mandrini *et al.* (1996), Démoulin *et al.* (1997), and Schmieder *et al.* (1997a), but never in the presence of BPs. The first such study involving BPs was performed by Aulanier *et al.* (1999b), where Hα flare kernels were associated with BPs. Such brightenings in a filament channel have also been observed in Ca II and correlated to BPs by Aulanier *et al.* (1998). However, in the case of filament BPs the order of magnitude of the energy deposit is likely to be less than in flares. Thus the Ca II kernels are not clear and no brightening is observed at all in Hα.

Schmieder *et al.* (1987, 1990) have shown observationally that some evaporation of the plasma occurs in flare kernels, leading to upwards motions. Typical blue shifts of 5 to 10 km s^{-1} were estimated from these observations in Hα and in UV (in a C IV line). This evaporation process has also been theoretically investigated in several works such as Forbes and Malherbe (1986) and Forbes and Acton (1996) and references therein.

Following the findings of Aulanier *et al.* (1998), we expect that evaporation occurs in the field lines anchored in the BPs, so that there are upward plasma flows along these field lines. As the amount of energy release is expected to be smaller than in flares, typical blue shifts $v_{\rm blue} < +10$ km s^{-1} may be observed.

5. Discussion

It has been shown by Aulanier *et al.* (1999a) that observations of the filament channel of 25 September 1996 in Hα (with the MSDP) were in accordance with the modeled magnetic configuration under the assumptions also used in this paper. In this Section, we discuss the relevance of the modeled features (described in Section 4.1) as well as their expected physical behavior (explained in Sections 4.2 and 4.3) with respect to the UV fine structures and their associated Doppler shifts observed in the Si IV line (with SOHO/SUMER) for the same filament channel (described in Sections 3.2 and 3.3).

5.1. Comparison of Si IV threads with computed field lines rooted in BPs

The comparison of the large computed field lines rooted in BPs and viewed from above, with the observed UV threads (see Figure 3) is presented in Figure 8. The model field lines shown are the ones which lie along the separatrix surface of the BPs. Thus we expect them to emit in UV, as is discussed in Section 4.2. We find that Si IV fine structures appear near many predicted locations, although not all. The orientation of these computed sheared field lines is in good agreement with the orientation of the bright threads. This is not only true for the set of the three southern brightenings forming the 'pincer' close to the strong western network brightening, but it is also valid for the long thread located at the center of the field of view of Figure 8(a).

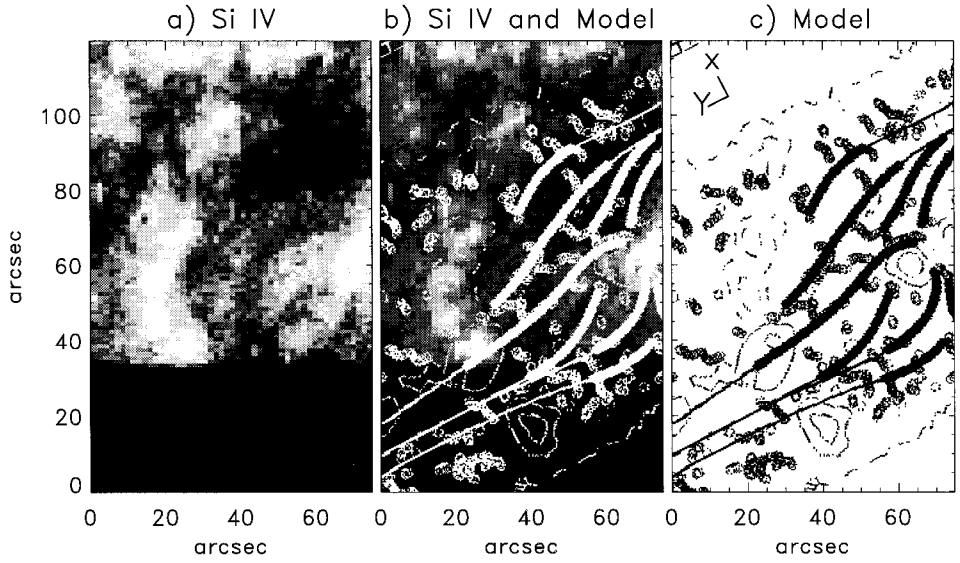

Figure 8. (a) A partial field of view of the filament channel observed in UV (Si IV) on 25 September 1996 between 11:23 and 11:52 UT. (c) A top view of the large field lines shown in Figure 7, computed from the SOHO/MDI magnetogram of 12:53 UT. The field lines are drawn darker between their footpoint and the altitude of 15 Mm, and thinner for their portion above 15 Mm. Some of these thick lines can be correlated to Si IV brightenings. This supports the hypothesis of ohmic heating along these field lines. On the photospheric plan, the thin solid lines correspond to isocontours of the vertical magnetic field of 8 and 24 G, dashed lines to -8 and -24 G, and the small circles to computed BPs. (b) is an overlay of (a) and (c) for direct comparison. The coordinate axes in the top left corner of (c) are for the same coordinate system as in Figures 6 and 7.

The strongest observed brightenings can be almost correlated to the thickest part of the drawn field lines, the portions which lie between the BP (at the photosphere) and slightly less than 15 Mm in the corona. Considering a typical height of 10 Mm, and looking at the perspective view of the field lines shown in Figure 7(c), these brightenings can be associated with typical lengths of $L_{\mathrm{Si\,IV}} = 20$ Mm along each field line. In other words, the plasma there is heated up to a temperature of the order of $T_{\mathrm{Si\,IV}}$ on a typical scale length of $L_{\mathrm{Si\,IV}}$. $L_{\mathrm{Si\,IV}}$ is much larger than L_{TR}, the typical length of the transition region, which has been evaluated be a few tens or hundreds of km theoretically (Vesecky, Antiochos, and Underwood, 1979) and observationally (see, e.g., Vial, 1990).

Consequently, as far as the comparison between the Si IV observations and the magnetic model is valid, plasma heating in the considered field lines is effective over the whole scale length of $L_{\mathrm{Si\,IV}}$. Thus the heating cannot be a stationary heating, as thermal conduction would rapidly reduce $L_{\mathrm{Si\,IV}}$ to typical values of L_{TR}. This is in agreement with the rapid variation of the Si IV intensity of these threads described in Section 3.2.

This non-stationary heating on an extended length is in accordance with the dissipation of currents layers in the field lines forming the BP separatrices discussed in Section 4.2. In this scenario, the currents are likely to be dissipated quite homogeneously in the separatrices, but they are probably not generated continuously. This implies variable motions of the photospheric magnetic polarities which are responsible for the presence of BPs.

In summary, the hypothesis of plasma heating in these field lines is supported by the observations, as these field lines are bright along a length of ≈ 20 Mm in a UV line with a typical temperature of formation of $T_{\mathrm{Si\,IV}} = 100\,000$ K. This indicates that the fine structures are formed along heated field lines rooted in 'bald patches' (and forming sheared arcades above the filament), rather than parts of a classical corona–chromosphere transition region (CCTR) which should normally be present in each of these field lines.

5.2. Evaporation scenario for Si IV blue shifts in the threads

The Si IV Doppler velocities associated to the bright UV threads are described in Section 3.3. Let us consider the threads forming the 'pincer' at the south-west of the SUMER field of view. As was mentioned previously, we were not able to calibrate the data, but instead set the average Doppler shift over the entire image to -7.8 km s^{-1}, a typical value for Si IV in the quiet Sun. We believe that our field of view is sufficiently large and this value is sufficiently well known so that this calibration is reliable to ± 3 km s^{-1} or better (see discussion in Section 2.1).

It is clear from Figure 5 that there are very weak red shifts in the brightest parts of the 'pincer', near the network brightening (North Box of Figure 5). As shown in Section 5.1, and according to the geometry of the computed field lines (discussed in Section 4.1 and shown in Figure 7(c)) this means that there are slow downflows of the plasma of $-10 \leq v_{\mathrm{red}} \leq 0$ km s^{-1} in the lowest part of the heated field lines. In these regions, the field lines are strongly bent so that they are nearly parallel with the photosphere ($0 \leq \theta \leq \pi/6$). This corresponds to typical lengths of 10 Mm along the field lines.

Because the plasma is frozen in the magnetic field, what is observed here is a combination of the plasma motions along the field lines (due to pressure gradients probably driven by thermal evolution) and the vertical displacement in time of the magnetic field itself (due to the evolution of the underlying parasitic polarities discussed by Aulanier *et al.* (1999a)). It is difficult to interpret the resulting observed plasma velocities in such a magnetic configuration. How these affect Hα Doppler shifts has already been discussed by Aulanier *et al.* (1999a).

However, we do note that the South Box in Figure 5 clearly shows some blue shifts in one of the parts of the threads in the 'pincer' where the associated field lines are more vertical (see Figure 7(c)). The measured velocities in the threads are $0 \leq v_{\mathrm{blue}} \leq +6$ km s^{-1}. In this region, Doppler velocities are dominated by the

plasma motions along the field lines, because these are closer to the vertical than in the case of the North Box in Figure 5.

Thus, there is evidence that vertical plasma upflows are observed in the higher parts of some threads. Moreover, the measured values of v_{blue} are in accordance with the values expected from an evaporation scenario (see discussion in Section 4.3). This interpretation of the fine-structure Doppler shifts would imply that the magnetic field structure and Doppler-shift mechanism differ in these areas from those in the network. However, further work will have to be done with other sets of observations before any conclusions can be made.

6. Conclusions

Our main findings with regard to the Aulanier and Démoulin model are: (1) There are fine structures in the Si IV emission near the filament. These features have similar orientations and locations to features predicted by the Aulanier and Démoulin model. The model predicts that such features will be visible in the UV in connection with locations where magnetic field lines rooted in parasitic polarities are tangent to the photosphere ('bald patches'). These field lines are part of the sheared arcade overlaying the filament, indicating that the UV fine structures are not a part of the regular chromosphere–corona transition region. (2) The bright fine structures are generally slightly red-shifted (-10 to 0 km s^{-1}). However, there is a bright blue-shifted area. This can be interpreted as evaporation due to heating by ohmic dissipation. Seen along a magnetic field line oriented near to the line of sight this would produce a blue shift.

In general, the Doppler values in Si IV follow the pattern, previously noted by Klimchuk (1987) for C IV, that areas with higher photospheric magnetic fields tend to be brighter and more red-shifted than areas with low field. On average the filament and nearby non-network areas show similar shifts. This is consistent with indications that the filament is mostly optically thin in Si IV. Although there may be some contribution to the velocity from the filament itself, most of the signal is probably from the filament channel transition region below the prominence rather than in the PCTR.

There would be a number of things which would help us further investigate the flows in the filament region. (1) Measurements with longer time exposures might help us pick out different Doppler components in the line profiles, allowing us to distinguish between the contributions of the filament and the regions below it. (2) Observations of lines likely to be more optically thick in filaments might give us better measurements of filament flows. (3) To adequately test the model, observations with more frequent magnetograms would be needed to study the evolution of the predicted fine structures.

Acknowledgements

We wish to thank all those who contributed the SOHO JOP 17 campaign. We also thank Dr S. Hill for assistance with the figures and Dr A. Poland and the referee for comments on the manuscript. The SUMER project is financially supported by DARA, CNES, NASA, and the ESA PRODEX programme (Swiss contribution). SUMER, CDS, and MDI are parts of SOHO, the Solar and Heliospheric Observatory, of ESA and NASA.

References

Aly, J. J. and Amari, T.: 1997, *Astron. Astrophys.* **319**, 699.
Aulanier, G. and Démoulin, P.: 1998, *Astron. Astrophys.* **329**, 1125.
Aulanier, G., Démoulin, P., van Driel-Gesztelyi L., Mein P., and DeForest C.: 1998a, *Astron. Astrophys.* **335**, 309.
Aulanier, G, Schmieder, B., Démoulin, P., Mein, N., van Driel, L., Mein, P., and Deforest C.: 1998b, in R. A. Harris , F. Moreno-Insertis, E. R. Priest (eds.), *A crossroads for European, Solar and Heliospheric Physics*, ESA, SP-417, p. 217.
Aulanier, G., Démoulin, P., Mein, N., van Driel-Gesztelyi, L., Mein, P., and Schmieder, B.: 1999a, *Astron. Astrophys.* in press.
Aulanier, G., Démoulin, P., Schmieder, B., Fang, C., and Tang, Y. H.: 1999b, *Solar Phys.* in press.
Billinghurst, M. N., Craig, I. J. D., and Sneyd, A. D.: 1993, *Astron. Astrophys.* **279**, 589.
Bommier V., Landi Degl'Innocenti E., Leroy J. L., and Sahal-Bréchot S.: 1994, *Solar Phys.* **154**,231.
Brekke, P., Hassler, D. M., and Wilhelm, K: 1998, *Solar Phys.* **175**, 349.
Bungey, T. N., Titov, V. S., and Priest, E. R.: 1996, *Astron. Astrophys.* **308**, 233.
Chae, J. C, Yun, H. S., and Poland, A. T.: 1998, *Astrophys. J. Suppl. Ser.* **114**, 151.
Chiuderi-Drago, F., Engvold, O., and Jensen, E.: 1992, *Solar Phys.* **139**, 47.
Démoulin, P.: 1998, in D. Webb, B. Schmieder, and D. Rust (eds.), 'New Perspectives on Solar Prominences', *IAU Colloq.* **167**; *Astron. Soc. Pacific Conf. Ser.* **150**, 78.
Démoulin, P. and Priest E. R.: 1989, *Astron. Astrophys.* **214**, 360.
Démoulin, P., Priest E. R., and Anzer U.: 1989, *Astron. Astrophys.* **221**, 326.
Démoulin, P., Hénoux, J. C., and Mandrini, C. H.: 1992, *Solar Phys.* **139**, 105.
Démoulin, P., Hénoux, J. C., Priest, E. R., and Mandrini, C. H.: 1996, *Astron. Astrophys.* **308**, 643.
Démoulin, P., Bagalá, L. G., Mandrini, C. H., Hénoux, J. C., and Rovira M. G.: 1997, *Astron. Astrophys.* **325**, 305.
Engvold O.: 1989, E. R. Priest (ed.), *Dynamics and Structure of Quiescent Polar Prominences*, Kluwer Academic Publishers, Dordrecht, Holland. p. 47.
Engvold, O., Tandberg-Hanssen, E., and Reichmann, E.: 1985, *Solar Phys.* **96**, 35.
Feldman, U., Laming, J. M., Mandelbaum, P, Goldstein, W. H., and Osterheld, A.: 1992, *Astrophys. J. Suppl. Ser.* **398**, 692.
Forbes, T. G. and Acton, L. W.: 1996, *Astrophys. J.* **459**, 330.
Forbes, T. G. and Malherbe, J. M.: 1986, *Astrophys. J.* **302**, L67.
Harrison, R. A. *et al.*: 1995, *Solar Phys.* **162**, 233.
Harrison, R. A. *et al.*: 1997, *Solar Phys.* **170**, 123.
Karpen J. T., Antiochos S. K., and DeVore C. R.: 1991, *Astrophys. J.* **382**, 327.
Klimchuk, J. A.: 1987, *Astrophys. J.* **323**, 368.
Koutchmy, O. and Koutchmy, S.: 1989, in O. von der Luhe (ed.) *Proc. 10th Sacramento Peak Summer Workshop, High Spatial Resolution Solar Observations*, NSO, Sunspot, p. 217.

Lemaire, P. *et al.*: 1997, *Solar Phys.* **170**, 105,
Low, B. C.: 1992, *Astrophys. J.* **399**, 300.
Low, B. C. and Wolfson, R.: 1988, *Astrophys. J.* **324**, 574.
Malherbe, J. M., Schmieder, B., Simon, G., Mein, P., and Tandberg-Hanssen, E.: 1987, *Solar Phys.* **112**, 233.
Mandrini, C. H., Démoulin, P., Van Driel-Gesztelyi, L., Schmieder, B., Cauzzi, G., and Hofmann, A.: 1996, *Solar Phys.* **168**, 115.
Martin, S. F. and McAllister, A. H.: 1996, in 'Magnetodynamic Phenomena in the Solar Atmosphere', *Proc. IAU Colloq.* **153**, 497.
Martin, S. F., Bilimoria, R., and Tracadas, P. W.: 1994, in R. J. Rutten and C. Schrijvers (eds.), *Solar Surface Magnetism*, Kluwer Academic Publishers, Dordrecht, Holland, p. 303.
Mein, P.: 1991, *Astron. Astrophys.* **248**, 669.
Mein, P., Schmieder, B., Malherbe, J.-M., Wiik, J. E., Engvold, O., Brekke, P., Zirker, J. B., Poland, A. I., Delaboudinière, J.-P., and Staiger, J.: 1998, in D. Webb) B. Schmieder, and D. Rust (eds.), 'New Perspectives on Solar Prominences', *IAU Colloq.* **167**; *Publ. Astron. Soc. Pacific* **150**, 135.
Meyer, J.-P.: 1985, *Astrophys. J. Suppl. Ser.* **57**, 173.
Moran, T.: 1999, in preparation.
Poland, A.: 1990, in V. Ruždjak and E. Tandberg-Hanssen (eds.), *Dynamics of Quiescent Prominences*, Springer-Verlag, Berlin, Vol. 363, p. 120.
Poland, A. I. and Tandberg-Hanssen, E.: 1983, *Solar Phys.* **84**, 63.
Schmieder, B.: 1989, in E. R. Priest (ed.), *Dynamics and Structure of Quiescent Solar Prominences*, Kluwer Academic Publishers, Dordrecht, Holland, p. 15.
Schmieder, B, Malherbe, J. M., Mein, P., and Tandberg-Hanssen, E.: 1984, *Astron. Astrophys.* **136**, 81.
Schmieder B., Forbes, T. G., Malherbe, J. M., and Machado, M. E.: 1987, *Astrophys. J.* **317**, 956.
Schmieder, B., Malherbe, J. M., Simnett G. M., Forbes, T. G., and Tandberg-Hanssen, E.: 1990, *Astrophys. J.* **356**, 720.
Schmieder, B., Aulanier, G., Démoulin, P., van Driel-Gesztelyi, L., Roudier, T., Nitta, N., and Cauzzi, G.: 1997a, *Astron. Astrophys.* **325**, 1213.
Schmieder, B., van Driel-Gesztelyi, L., Wiik, J. E., Kucera, T., Thompson, B., DeForest, C., StCyr, C., and Simnett, G. M.: 1997b, in A. Wilson (ed.), *Fifth SOHO Workshop: the Corona and Solar Wind Near Minimum Activity*, ESA, SP- 404, p. 663.
Titov, V. S., Priest, E. R., and Démoulin, P.: 1993, *Astron. Astrophys.* **276**, 564.
van Driel-Gesztelyi, L. Schmieder, B., Martens, P., Zarro, D., DeForest, C., Thompson, B., Aulanier, G., Démoulin, P., StCyr, C., Burkepile, J., White, O. R., Kucera, T., Nitta, N., Hanaoka, Y., Mein, P., Malherbe, J.-M.: 1997, *Annales Geophysicae Supplement*, Part III, Space & Planetary Sciences, Supplement III to Volume 16, C918.
van Driel-Gesztelyi, L., Schmieder, B., Aulanier, C., Démoulin, P., Martins, P. C. H., Zarro, D., DeForest, C., Thompson, B., St.Cyr, C., Kucera, T., Burkepile, J. T., White, O. R., Hanaoka, Y., and Nitta, N.: 1998, in D. Webb, B. Schmieder, and D. Rust (eds.), 'New Perspectives on Solar Prominences', *IAU Colloq.* **167**; *Astron. Soc. Pacific Conf. Ser.* **150**, 366.
Vekstein, G. E., Priest, E. R., and Amari, T.: 1991, *Astron. Astrophys.* **243**, 492.
Vesecky, J. F., Antiochos, S. K., and Underwood, J. H.: 1979, *Astrophys. J.* **233**, 987.
Vial, J. C.: 1990, in V. Ruždjak and E. Tandberg-Hanssen (eds.), *Dynamics of Quiescent Prominences*, Springer-Verlag, Berlin, Vol. 363, p. 106.
Wilhelm, K. *et al.*: 1995, *Solar Phys.* **162**, 189.
Wilhelm K. *et al.*: 1997, *Solar Phys.* **170**, 75.